

A DYNAMICAL MODEL OF A GAS MICROTURBINE GENERATOR FOR DISTRIBUTED GENERATION

Chiara Boccaletti, Stefano Elia, Eleonora Nisticò
Department of Electrical Engineering
University of Rome "La Sapienza" - Via Eudossiana 18, 00184 Rome, Italy
Tel. +39 06 44585762 Fax +39 06 4883235
e-mail: chiara.boccaletti@uniroma1.it

ABSTRACT

A dynamical model of a microturbine and its control systems has been set up and developed in the Simulink[®] environment. In particular, the model of the electrical part, not available in the literature, was conceived by the authors. Experimental parameters from an actual cogeneration plant have been implemented in the model, allowing the accurate analysis of the dynamic behaviour of the system, with particular reference to the connection with the grid. Finally, some transient conditions are simulated in different operation modes and the results are discussed.

KEY WORDS

Gas microturbines, Modelling, Distributed generation, Cogeneration.

1. Introduction

Small power plants (up to some tens of MWs) for the production of electricity or cogeneration, installed close to industrial plants, commercial or residential buildings, are indicated as distributed generation (DG). Small, modular electricity generators sited close to the customer load can enable utilities to defer or eliminate costly investments in transmission and distribution. In the last years, the demand for connection of small power plants to the distribution grid strongly increased. Aiming to reduce the cost and increase the efficiency, electric companies are more and more interested in developing small cogeneration systems. These can be installed in single configuration, to meet a single customer's demand, or in multiple configuration, contributing in a coordinate way to meet the demand of several customers. Finally, in both single or multiple configuration, cogeneration systems can be integrated in the electric grid. However, connecting a distributed power system to the electricity grid has a potential impact on the safety and reliability of the grid itself. Thus, a new approach has to be adopted to face the increase of the short-circuit power, the lack of selectivity of the protections, the different voltage profiles, power flows, and voltage regulation, the service quality, etc.. In Italy, medium- and high-voltage grids are usually designed and managed to be passive and to be operated "radially". The few plants of DG connected to

the grid are disconnected in case the grid is not fed. Indeed, to improve the service continuity and to fully exploit the DG features, the islanding operation mode should be allowed in the medium voltage (MV) line, in which a distributed generator energizes a portion of a distribution system when the rest of the system is de-energized. This can create safety hazards and damage equipment. Presently, it is not allowed neither in Italy nor in many other countries. Technologies for distributed electricity generation include wind, solar, biomass, fuel cells, gas microturbines, hydrogen, combined heat and power, and hybrid power systems. Gas microturbines are compact systems varying from 30 kW up to 200 kW with a quite good efficiency. The exhaust gas is used for combustion air pre-heating and for water heating. The hot water produced in cogeneration can be used, for instance, to feed absorption chillers. In the following sections a dynamical model of a gas microturbine, developed by the authors in the Simulink[®] environment, is described. The behaviour of a power generation system during transients is analysed and discussed.

2. High-speed microturbines for cogeneration

High-speed gas microturbines are suitable for cogeneration applications, because of their power size and of the exhaust gas temperature. Usually, the fuel is methane, but also gas oil is used. The power sizes available in the market vary from 30 kW up to 200 kW; the rated speed of the electric generator may vary between 50000 and 150000 rpm. A typical scheme of such systems is shown in Fig. 1. If the system is in islanding mode, the reference quantities for the control signals are frequency and voltage; if the system is in parallel with a infinite power electric network, these quantities are fixed, therefore the reference quantities are the active and reactive powers. The interface has the function of 1) control, 2) measurement, 3) protection. The converter includes 1) a diode rectifier, 2) an inverter, 3) a transformer connecting the converter to the grid, 4) AC and DC filters, 5) connection devices between the turbine and the rectifier, 6) protection devices, 7) control devices. In case of insertion in MV or high voltage lines, the transformer is necessary to reduce the voltage at the level required by the electronic components of the converter.

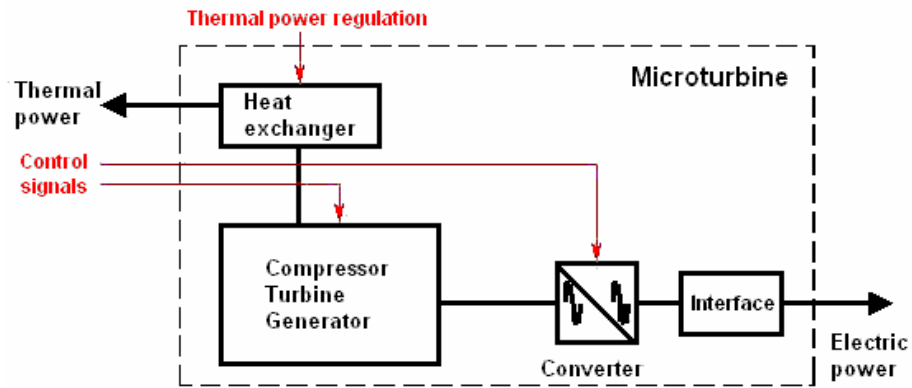


Figure 1. Scheme of a gas microturbine power generator.

The advantages of microturbines in comparison with internal combustion engines can be resumed as follows:

- plain structure of rotating parts;
- reduced maintenance costs;
- low emissions;
- long intervals between maintenance interventions;
- high temperatures (suitable for cogeneration);
- operation flexibility;
- control flexibility.

3. The Experimental Facility

In order to analyse the possibilities of the gas microturbine technology, a small cogeneration plant has been studied. It consists of a power generator, an absorption chiller, and other thermal and electric loads (Figs. 2, 3). The thermal power of the microturbine is 300 kW, the electric power is 45 kW. The scheme of the electric circuit is shown in Figure 4. It consists of a permanent magnet synchronous generator, a 2 kHz rectifier, a booster chopper regulating the inverter in-voltage, an inverter, filters, and a starting circuit with batteries and an auxiliary chopper. The system can operate in parallel with the grid or in islanding mode. In both cases the turbine follows the inverter adjusting the power delivery on the DC line, at constant rotation speed. The absorption heat pump has a rated power of 180 kW in cooling mode (summer) and 160 kW in heating mode (winter). The working fluid is water-lithium bromide.

4. Experimental tests

Some experimental tests have been performed in order to verify the microturbine performance and to analyse its behaviour in relation to the grid, both in normal operating conditions and in fault conditions.

In particular, the following test have been performed:

- response to a load step change;
- behaviour in islanding mode;
- operation with the auxiliary devices disconnected;
- response to given external disturbances.

All tests aimed to characterise the electric response at the end connections. From the electric point of view, the

response of the system to the dynamical loads was extremely fast and efficient. This is due to the de-coupling of the mechanical speed and the feeding frequency, operated by the static converter. In the following, some results are reported.



Figure 2a, b. Views of the experimental facility.

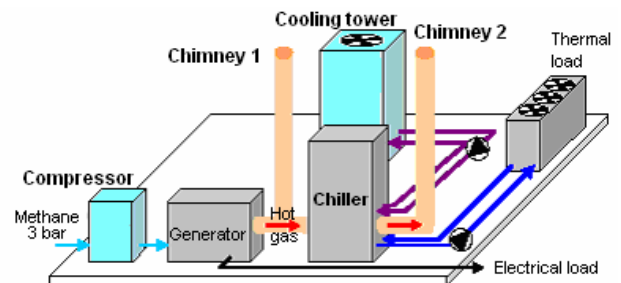


Figure 3. Sketch of the experimental facility.

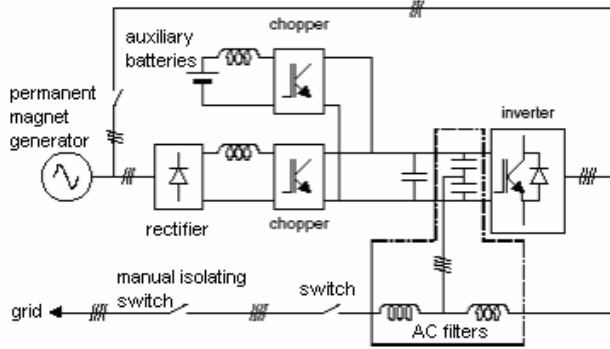


Figure 4. Scheme of the electric system.

A first test consisted in the insertion of a resistive load in islanding mode. Figure 5 shows the voltage (red) and current (green) curves, for a load of 22 kW and 38.5 kW, respectively. The voltage drop is recovered in few cycles. As to the utility grid, the transient has no influence on the behaviour of the generator in islanding mode, even when the load is close to the rated power.

In this microturbine generation system, it is not possible to switch to the islanding mode automatically, in case the grid fails. In fact, the control logic cannot be varied from grid-parallel to islanding, while the generator is running. However, for safety reasons, when a protection opens and a part of the line remains isolated it must be ensured that the turbine is excluded from this area, except for the islanding part. Therefore, some tests have been performed opening the isolating switch between the grid and the plant, when the delivered power was close to the local loads. In this case, one could figure out the inverter remains active, at least for a while, even if the control logic does not change. In Figure 6a, b, c three cases are reported, in which the inverter remains active no more than a second before it shuts off and disconnect. The load is 22 kW, the power is fixed at 25, 20 and 30 kW, respectively. For the case in which the difference between the load and the power previously delivered is the largest, the inverter shuts off almost instantaneously. The frequency variations are shown in Fig. 7, when the protections relevant to voltage and frequency cause the block at 1.1 s.

The above results are not sufficient to ensure a portion of the line is not fed in particular load conditions. A suitable co-ordination between the inverter and the grid

protections is required. Moreover, the control logic must be modified if the plant has to be switched automatically to the islanding condition. Further tests showed that, if the interface device is switched on and off in very short time intervals (250÷300 s), the inverter does not shut off and resumes the synchronism with the grid, even if the phase angle is large (see Fig. 8). Thus, it should be not necessary to disconnect the generator from the grid in case of fault, with an appropriate control logic. The analysis and implementation of the voltage and power control in the different operating conditions, keeping some internal quantities fixed (e.g. the mechanical rotating speed), was the subject of the second phase of the research activity.

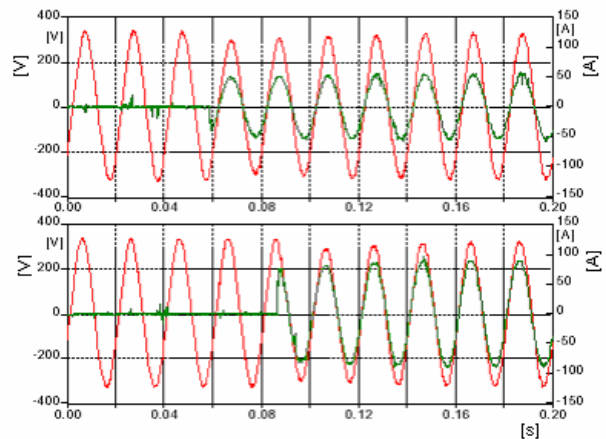


Figure 5a, b. Response to a load step change: voltage (red) and current (green) curves for a resistive load of 22 kW (upper diagram) and 38.5 kW (lower diagram), respectively.

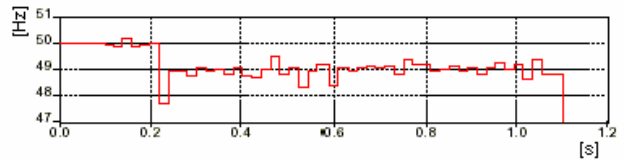


Figure 7. Frequency curve after the isolating switch is opened. The inverter is blocked at 1.1 s.

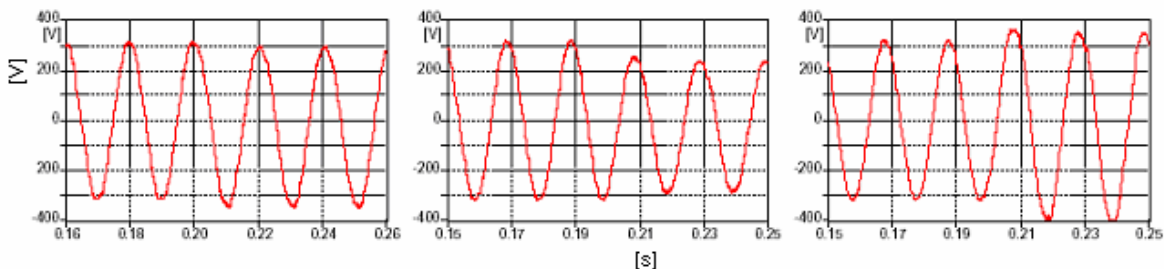


Figure 6a, b, c. Voltage curves after the isolating switch is opened when the power is fixed at 25, 20 and 30 kW, respectively.

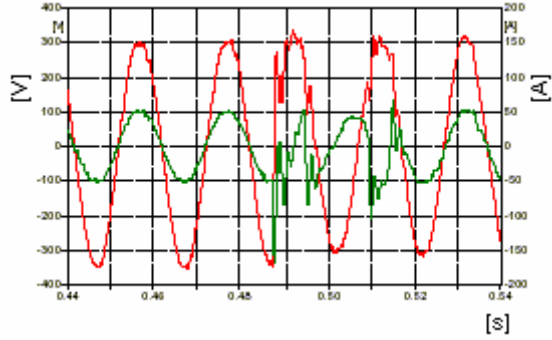


Figure 8. Voltage (red) and current (green) in one phase after the isolating switch is closed again.

5. The dynamical model

In order to describe and analyse the electrical and mechanical behaviour of the microturbine during transients, a model of the whole generator has been conceived and set up. Firstly, the fundamental equations of the electromechanical system have been individuated. Then, they have been implemented in the Simulink[®] environment. The necessary experimental parameters have been drawn from the experimental facility described in the previous sections.

5.1 The microturbine electric system

The electric circuit of the generator is shown in Fig. 9. The diode bridge rectifies the high-frequency AC from the generator, the booster change the voltage from v_{c1} to v_{c2} , and the inverter transforms the DC in a 50 Hz AC. The generator is a salient-pole permanent magnet synchronous machine.

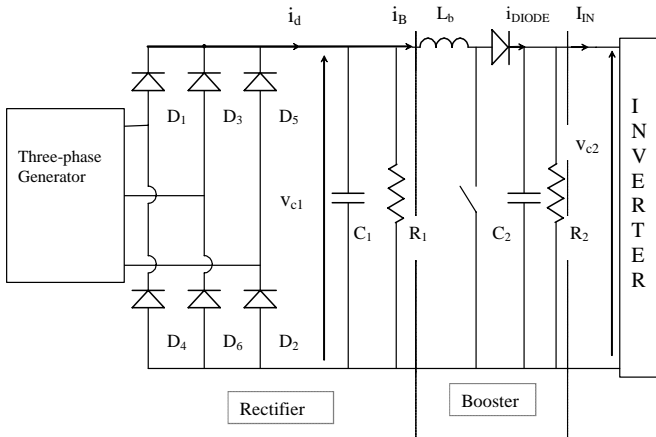


Figure 9. Scheme of the electric system

For the rectifier, three different models have been used, according to the value of v_{c1} . If v_{c1} is large, one upper diode and one lower diode conduct at the same time, or none; if v_{c1} has a little value, there are intervals in which 2 diodes conduct and intervals in which 3 diodes conduct at the same time; for intermediate values of v_{c1} , 0, 2 or 3 diodes can conduct at the same time. The results obtained with these models have been compared with the results obtained simulating the rectifier circuit with SPICE[®]. The

agreement is quite good, as shown in the diagram of Fig. 10, where I_{sc} is the short-circuit current. Finally, the three curves of Fig. 10 have been approximated with two parabolas.

To model the booster, the condition $v_{c2} > v_{c1}$ has been fixed. Choosing a short switching period T_s , one can assume v_{c2} and v_{c1} are constant when the switch is closed (T_{on} in Fig. 11). In this case, $i_{DIODE} = 0$ and i_b increases linearly with slope v_{c1}/L_b , as shown in Fig. 11.

In the model, some quantities can be approximated by their mean value in T_s , since T_s is very short.

After some calculations, the equations describing the system of generator, rectifier and booster are the following.

$$C_1 \cdot \frac{dv_{c1}}{dt} = I_d' \cdot \frac{v_{c1}}{R_1} - I_b = \frac{\eta_r \cdot a_2 \cdot v_{c1}^2}{\sqrt{2} \cdot 3 \cdot \sqrt{2} \cdot k_s \cdot \omega_{el}^2 \cdot L_c} + \frac{\eta_r \cdot a_1}{\sqrt{2} \cdot \omega_{el} \cdot L_c} \cdot \frac{v_{c1}}{\sqrt{3}} + \eta_r \cdot \frac{a_0 \cdot k_s}{L_c} \cdot \frac{v_{c1}}{R_1} - I_b \quad (1)$$

$$L_b \cdot \frac{dI_b}{dt} = v_{c1} - \alpha \cdot v_{c2} \quad (2)$$

$$C_2 \cdot \frac{dv_{c2}}{dt} = \alpha \cdot I_b - I_{IN} - \frac{v_{c2}}{R_2} \quad (3)$$

C_1 and C_2 , R_1 and R_2 being the capacities and the resistances of Fig. 9, respectively; $I_d' = I_d \cdot \eta_r$ ($\eta_r < 1$); k_s being the constant of proportionality between generator voltage E_s (rms value of emf) and pulsation ω_{el} ; a_2 , a_1 , and a_0 being the coefficients of the parabolas approximating the curves of Fig. 10; I_{IN} being the current flowing into the inverter; α being the constant of proportionality between the mean value of i_{DIODE} and I_b ($I_b = \bar{i}_b$; $i_b = i_B$).

The inverter is a VSI with PWM. Rms output voltage is related to input voltage v_{c2} through parameter $m \leq 1$. The shape of the feedback current can be modified acting on the inverter switches by means of an appropriate circuit. The latter can be assumed to be very fast, so that the variations of the control current are instantaneously applied to the output current. Defining $\delta = \tan^{-1}(V_x/V_r)$, the equations describing the inverter behaviour (real part of output phase current I_r and output power P_{el}) can be written

$$I_r = I_{set} \cdot \cos(\delta + \varphi); \quad I_{set} = \sqrt{I_r^2 + I_x^2} \quad (4)$$

$$P_{el} = V_{C2} \cdot I_{IN} \cdot \mu_{inv} = \sqrt{3} \cdot (V_r \cdot I_r + V_x \cdot I_x); \quad V_{inv} = \sqrt{V_r^2 + V_x^2} \quad (5)$$

where I_{set} is the module of the inverter output phase current, V_r , V_x are the real and imaginary part of output concatenated voltage V_{inv} , respectively, φ is the phase angle, I_{IN} is the inverter input current, and μ_{inv} is the efficiency of conversion DC/AC.

The equation of momentum for the generator is

$$J \cdot \omega = C_{mec} - C_{el} \quad (6)$$

being J the momentum of inertia of the rotating mass, $C_{mec} = C_t - C_c$ being the mechanical torque of the turbine subtracted of the compressor load, and C_{el} being the electrical torque.

The output power of the synchronous generator entering the bridge is

$$P_{gen} = \frac{v_{c1} \cdot I_d'}{\eta_r} = v_{c1} \cdot I_d \quad (7)$$

where I_d' can be substituted by the same expression used in Eqn (1).

In conclusion, the model consists of equations (1), (5), (6), (7), which can be normalized with respect to reference values V_{ref} , I_{ref} , $P_{ref} = V_{ref} I_{ref}$, ω_{ref} .

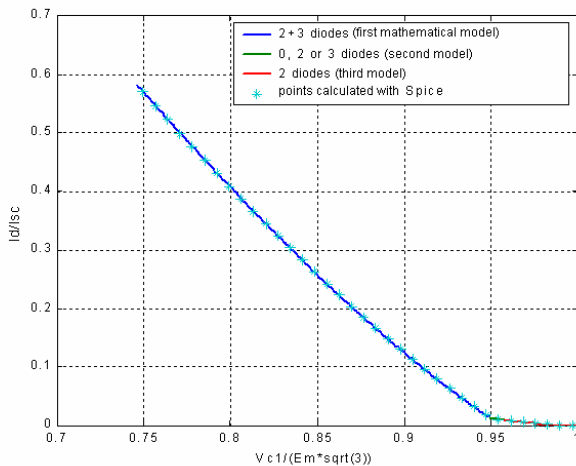


Figure 10. I_d/I_{sc} versus v_{c1} . The coloured lines are calculated with three different mathematical models, the light blue stars are the points calculated by SPICE®

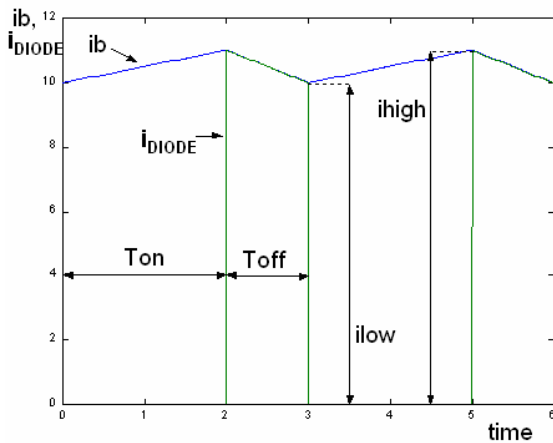


Figure 11. Booster current i_b (blue) and i_{DIODE} (green) versus time.

5.2 Implementation of the Model in the Simulink® Environment

The normalized equations describing the whole system have been implemented in the Simulink® environment, together with all necessary control systems.

The latter are:

- speed control;
- control of the booster voltage;
- control of the generated power for operation in parallel with the grid;
- control of the load voltage in islanding.

In the model, a manual isolating switch (see Fig. 4) allows the commutation from the parallel mode to islanding.

The Matlab- Simulink® model of the microturbine and the control system is shown in Fig. 12. In the figure, the position of the manual isolating switch corresponds to the islanding condition.

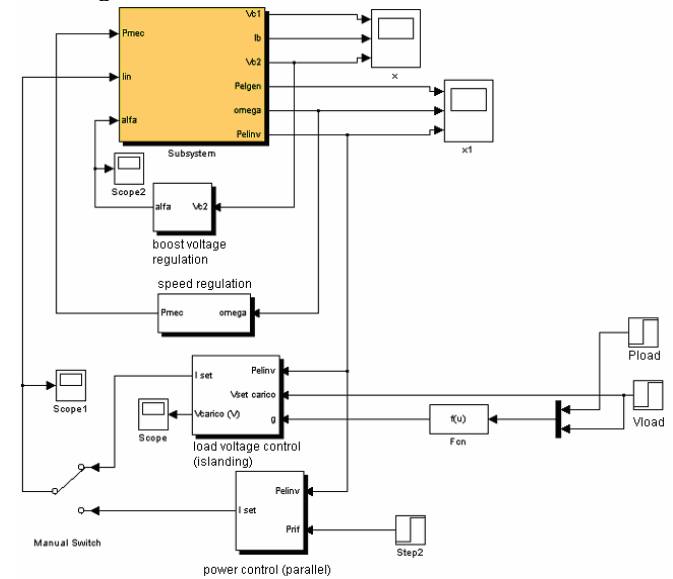


Figure 12. Matlab- Simulink® model of the microturbine and the control system

6. Simulation results

Some tests have been performed using the dynamical model described in the previous section. In the following, the results of two different tests are reported.

6.1 Step change of the generated power in the parallel mode

When the turbine is connected in parallel with the grid, the power delivered to the grid corresponds to the inverter output power, initially 40 kW. If this reference power P_{ref} is changed abruptly from 40 to 35 kW at time $t=10$ s, v_{c1} , v_{c2} , and I_b vary as shown in Fig. 13. The curves of P_{el} , mechanical rotating speed ω , and inverter output power P_{inv} are reported in Fig. 14. When the power demand, that is, the electrical load decreases, the turbine accelerates temporarily. Under the action of the regulator, the speed assumes again the initial value. The generator and the inverter follow immediately the power variation. The regulator of the booster voltage make v_{c2} return to the initial value.

6.2 Step change of the load in the islanding condition

For the sake of simplicity, be the load a resistive load with $R = 4 \Omega$, which requires $P_{load} = 40$ kW at a voltage of 400 V. If R is increased to 8Ω abruptly, the variation of

the mechanical and electrical quantities are those shown in Figures 15 and 16.

7. Conclusion

A dynamical model of a gas microturbine suitable for cogeneration applications has been developed and set up. Some transients have been analysed both in parallel with the utility grid and in islanding condition.

The model reaction to step variations of the generated power or the load is efficient and fast. When the load changes, the system varies the rotating speed and the generator power. If the load decreases, the generator speed increases and the inverter input current decreases, with different time constants. In particular, the reaction to speed changes can take tens of seconds, while the variation of the electrical quantities is much more rapid (less than 1 s).

8. Acknowledgements

The authors are in debt with Prof. Ezio Santini for helpful discussion.

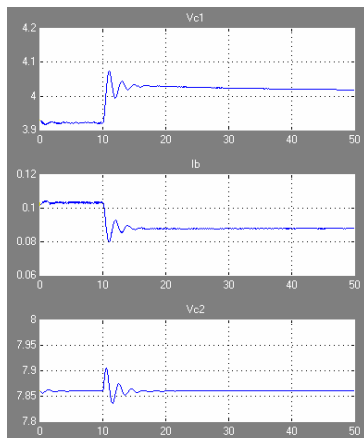


Figure 13. v_{c1} , I_b , and v_{c2} versus time for a step power change at $t = 10$ s.

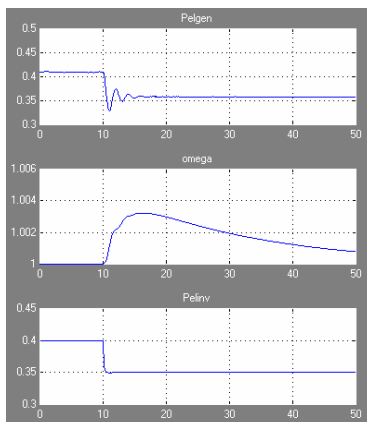


Figure 14. P_{el} , ω and inverter output power versus time for a step power change at $t = 10$ s.

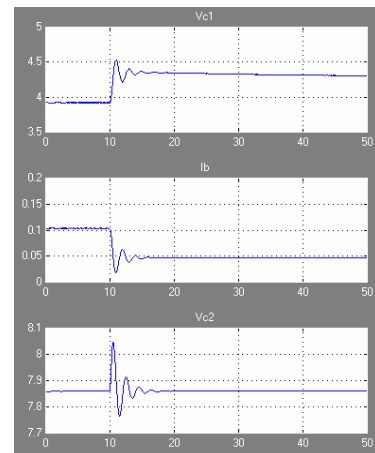


Figure 15. v_{c1} , I_b , and v_{c2} versus time for a step load change at $t = 10$ s.

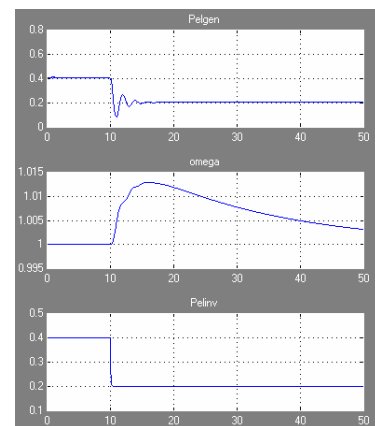


Figure 16. P_{el} , ω , and inverter output power versus time for a step load change at $t = 10$ s.

References

- [1] S.A. Papathanassiou, Technical Requirements for the Connection of Dispersed Generation to the Grid, *IEEE Power Society Summer Meeting*, 2, 2001.
- [2] P.P. Backer, R.W. de Mello, Determining the impact of Distributed Generation on Power Systems: Part 1, *Proc. IEEE PES Summer Meeting*, 3, Seattle (USA), 2000, 1645-1656.
- [3] S. Barsali, M. Ceraolo, P. Pelacchi, D. Poli, Control techniques of dispersed generators to improve the continuity of electricity supply, *IEEE Power Engineering Society Winter Meeting*, 2, NY, USA, 2002, 789-794.
- [4] R. Caldon, A. Scala, R. Turri, *Grid-connected Dispersed Generation: investigation on anti-island protections behaviour*, (University of Padova, Italy).
- [5] S. Barsali, M. Ceraolo, R. Giglioli, P. Pelacchi, Microturbines for dispersed generation, *Cired*, Nice, France, 1999.
- [6] S. Wall, Performance of Inverter Interfaced Distributed Generation, *IEEE/PES Transmission and Distribution Conference and Exposition*, 2, 2001.
- [7] J.C. Park, *Modeling and simulation of selected distributed generation sources and their assessment*, (MS thesis, Virginia University, Morgantown, WV, 1999).